The CDR method: Chapter 2 of a thesis in progress

Chuck Sword

ABSTRACT

The method of Controlled Directional Reception, developed over the last several decades in the Soviet Union, is based on picking traveltimes and ray parameters from short-base slant stacks. The slant stacks can be carried out over common-shot and common-geophone gathers, or over common-midpoint and common-offset gathers. Once the parameters have been picked, they can be used in imaging and velocity analysis. Imaging methods include time migration and depth migration. In addition, each set of picked parameters contains enough information to determine an average velocity, and with some care, this velocity can be used in the imaging. Stereo pairs can be formed, with velocity as the third dimension.

OVERVIEW

The method of Controlled Directional Reception (CDR) was first developed by an American, Frank Rieber, in the 1930's (Rieber, 1936). This method, in its most elementary form, consisted of carrying out slant stacks (linear stacks along lines of different slope (Schultz and Claerbout, 1978)) over a short range of offsets. Rieber called the resulting slant-stacked traces sonograms. The sonogram method did not receive a great deal of attention in the United States, but it was extensively developed, over the course of five decades, in the Soviet Union, under the name CDR. Dr. L.A. Riabinkin is the Soviet scientist whose name is most closely linked with this development (Hermont, 1979); he was always scrupulous about giving Rieber credit for the original idea of CDR. As seismic recording technology and processing techniques grew more sophisticated, so too did the CDR method. The most recent Soviet refinements to CDR take advantage both of computerization and of the dense coverage afforded by modern recording methods. Despite these refinements, Soviet geophysicists have not been able to take advantage of the full power of CDR, because of the difficulty they have in gaining access to adequate computer facilities. Thus, some of the methods I will describe are not similar to those that are used in the Soviet Union, and I will make no real attempt to describe present-day Soviet CDR techniques, except as they have been incorporated into my own approach.

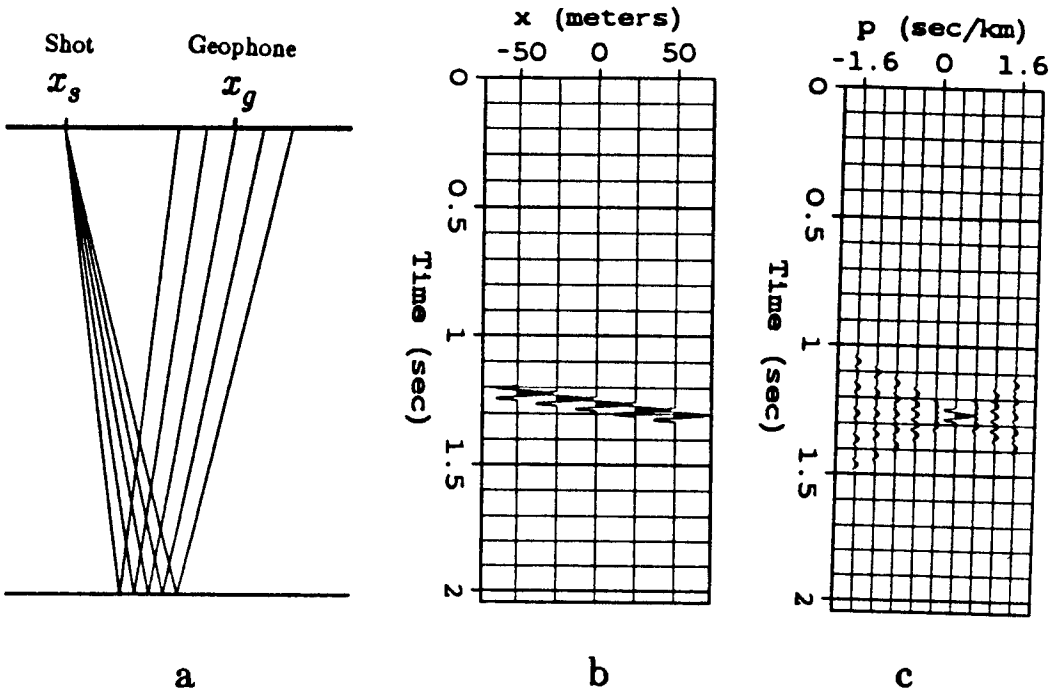

FIG. 1. Determining ray parameters. Panel (a) shows how a short-base common-shot gather might be collected in the field. Panel (b) shows the outcome of this seismic experiment (notice that the horizontal coordinate in this figure has its origin at location x_g). Panel (c) shows the result of slant stacking this data; from the slant-stack section it is possible to determine the ray parameter p_g (defined as $\Delta t/\Delta x_g$) and traveltime t of the reflection event.

Automated picking of slant stacks

The CDR method is based on the automated picking of pre-stack reflection seismic data; the goal of this picking is to obtain certain seismic parameters (Riabinkin et al., 1962). One of these picked parameters is traveltime (the time it takes a wave to travel from the source to the receiver); another is ray parameter, defined as the change in traveltime as the position (of the shot, receiver, or both) varies. The most useful ray parameters, for the purposes of tomographic velocity inversion, are the shot ray parameter (defined as the change in traveltime as shot position is varied, while the geophone position is held constant), and the geophone ray parameter (defined as the change in traveltime as the geophone position is varied, while the shot position is held constant).

In the CDR method, the ray parameters are not determined by picking traveltimes and directly measuring the change in traveltime with respect to position ($\Delta t/\Delta x$) . Instead, a gather of nearby traces is formed, and slant-stacking is performed. The gather is thus transformed from x–t to p–τ space, where p is the ray parameter. On such a p–τ gather, the point of maximum amplitude is easily picked, and the position of this maximum directly gives the ray-parameter (p) and traveltime (τ) information. Figure 1 shows how ray-parameter information (in this case, the geophone ray parameter) can be picked after slant-stacking.

Note that the ray-parameter and traveltime information can easily be picked by an automated algorithm. Since individual peaks are sought, rather than, for instance, continuous horizons, the algorithm can be comparatively simple. Note also that the CDR method is applied to pre-stack, unmigrated data.

Reciprocal parameters

The ultimate goal of the CDR method (or at least, of my application of the method), is to determine the parameters of particular reflection events. There are five parameters that will prove essential in CDR tomographic inversion: shot position x_s, geophone position x_g, shot ray parameter p_s, geophone ray parameter p_g, and traveltime t. It is possible to pick additional parameters as well, such as amplitude, mean wavelength, and so on, but these do not necessarily play a role in the inversion.

In Soviet geophysical terminology, approaches that simultaneously use the shot and geophone ray parameters are known as "reciprocal-point" methods. Thus, I shall refer to the five parameters x_s, x_g, p_s, p_g, and t, as the "reciprocal parameters". There is some overlap between the method of reciprocal points and the CDR method, since the CDR method (meaning slant stacks plus picking) is often used to pick the reciprocal parameters. But there are other techniques that can be used to determine these parameters. For instance, it is possible to perform a double slant stack, to determine p_s and p_g simultaneously (Harlan and Burridge, 1983; Pan and Gardner, 1986). It is possible to perform slant stacks over midpoint and offset rather than over shot and geophone coordinates. And in one technique, not directly related to CDR, the traveltime and dip are measured at a point on a zero-offset section, and through conventional velocity analysis, the stacking velocity is determined at that point. This information is converted into the five parameters (x_s, x_g, p_s, p_g, t) that are used in the tomographic approach (Glogovskii et al., 1979).

Velocity and displays

Once the five reciprocal parameters have been found by one means or another, they can be used to determine an effective velocity (Puzyrev, 1979; Urupov and Levin, 1985), which is similar in concept to RMS velocity. Each set of reciprocal parameters will thus have associated with it an average velocity. The effective velocities can be used, with the reciprocal parameters, to produce a rough migrated section, even before the exact interval velocity structure has been determined. This migrated section will not look like a conventional migrated section; it will be a dip-bar section (a picture made up of small dipping line segments). Stereo display techniques can be used to produce 3-dimensional displays of migrated data, where the two "flat" dimensions are the conventional midpoint and traveltime, while the third dimension, into the plane of the display, represents effective velocity. Such a stereoscopic display makes it easier for the interpreter to distinguish low-velocity phenomena (multiples, for instance) from high-velocity phenomena (primaries).

Velocity filtering

The effective velocities can be used in velocity filtering as well. For instance, all water-velocity events below the depth of the sea floor can be filtered out. It is fortunate that this capability for velocity filtering exists, since my tomographic inversion technique is not able, by itself, to distinguish between primary reflections and multiples. In order to achieve an accurate velocity inversion, it is necessary to eliminate all sets of reciprocal parameters associated with multiple reflections.

CDR PICKING METHODS

The goal of the CDR method (or rather, the goal of that aspect of the method that I have chosen to use), is to determine, at a given point, three basic parameters from the seismic data: shot ray parameter (p_s), geophone ray parameter (p_g), and traveltime (t). Two other parameters are specified as well: shot position (x_s), and geophone position (x_g). These last two parameters are obtained directly from the geometry of the seismic survey.

These five parameters can be determined using the "classical" CDR approach: slant stack over a gather of several traces, and look for peaks (maxima or minima) to pick (Riabinkin et al., 1962). This approach I will term a *direct* picking method. Several *indirect*, non-CDR, picking methods exist as well.

DIRECT PICKING METHODS

The parameters p_s and p_g can be picked directly, or they can be derived from other, related information (information obtained by slant stacking common-offset and common-midpoint gathers, for instance). And if a preliminary normal-moveout correction is applied to the data, the picked data are less likely to be aliased.

Picking p_s and p_g

In the simplest case of direct picking, the parameters p_s and p_g (respectively, the shot and geophone ray parameters) are picked. Suppose it is desired to determine the ray parameters of a reflected wave that has traveled from shot location x_s to receiver location x_g. To determine p_g, a gather is formed that contains all the traces that were recorded by receivers at or near position x_g, when the shot was fixed at position x_s. A slant stack is then performed over this gather. Likewise, to determine p_s, a gather is formed containing all traces recorded at the fixed geophone position x_g, while the shot was at or near location x_s, and this gather is slant stacked.

In mathematical terms, let the entire recorded wavefield be described by $u_{ij}(t)$, where $i = 1, 2, 3..., n_{\text{shot}}$, and $j = 1, 2, 3..., n_{\text{geo}}$. Here i is the shot location number, j is the geophone location number, n_{shot} is the number of shots, and n_{geo} is the number of geophones. Suppose that the distance between shots is Δs, and the distance between geophones is Δg. Suppose, furthermore, that n_{base} traces are to be summed together to form the slant stack. Typical values of n_{base} range from 7 to 15. The greater the value of n_{base}, the higher the signal-to-noise ratio of the slant stack, and the greater the resolution in p, but the lower the spatial resolution.

The slant-stacked wavefield $r_{g(m)}(t)$ used to find p_g is produced according to the formula

$$r_{g(m)}(t) = \sum_{k=-n_{\text{bh}}}^{n_{\text{bh}}} u_{i(j+k)}(t + mk\Delta p\Delta g), \tag{1}$$

where $r_{g(m)}(t)$ is the slant-stacked wavefield, m depends on the ray parameter p_g according to the formula $p_g = m\Delta p$, i is the shot index, j is the geophone index, and $n_{\text{bh}} = (n_{\text{base}} - 1)/2$. The other variables are as previously defined. Figure 1 shows the results of carrying out such a slant stack.

It is possible to make the slant-stack peaks sharper by applying semblance weighting to

the slant stack (Kong et al., 1985; Stoffa et al., 1981). This semblance weighting is most effective when there is only one dip present at a particular time. The semblance weighting function $w_m(t)$ is

$$w_m(t) = \frac{\left[\sum_{k=-n_{\rm bh}}^{n_{\rm bh}} u_{i(j+k)}(t + mk\Delta p\Delta g)\right]^2}{(2n_{\rm bh}+1)\sum_{k=-n_{\rm bh}}^{n_{\rm bh}} u^2_{i(j+k)}(t + mk\Delta p\Delta g)}. \tag{2}$$

It is useful to smooth this weighting function in time, before applying it to the slant stack. If $w'_m(t)$ is defined to be the smoothed version of $w_m(t)$, then the slant stack $r_{g(m)}(t)$ is weighted according to

$$r_{g(m)}(t) = w'_m(t) \cdot r'_{g(m)}(t), \tag{3}$$

where $r'_{g(m)}(t)$ is the original unweighted slant stack.

Equations (1) and (2) define the slant-stacking and semblance procedures when u_{ij} is a continuous function of time. In practice, u_{ij} is discretized in time, as is the output, $r_{g(m)}$. In order to convert between discretized and continuous time, an interpolation scheme should be used.

The slant-stack wavefield $r_{s(m)}(t)$, used for finding p_s, is produced similarly:

$$r_{s(m)}(t) = \sum_{k=-n_{\rm bh}}^{n_{\rm bh}} u_{(i+k)j}(t + mk\Delta p\Delta s). \tag{4}$$

A semblance weight can be applied to $r_{s(m)}(t)$; the formulas, analogous to those in equations (2) and (3), will not be given here. Once the common-geophone and common-shot gathers have been transformed to $r_{s(m)}(t)$ and $r_{g(m)}(t)$ slant-stack panels respectively, the picking process can begin. This process consists of looking for peaks (maxima and minima) on the slant-stack panels. A particular reflection event should have the same traveltime on both $r_{s(m)}(t)$ and $r_{g(m)}(t)$, since both panels are produced from gathers centered on the trace whose geophone is located at x_g and whose shot is located at x_s. So if peaks having identical traveltimes are found on both the $r_{s(m)}(t)$ and $r_{g(m)}(t)$ panels, it is likely that they correspond to the same event. I use a picking method loosely based on a method developed in the Soviet Union (Rapoport, 1977).

Determining p_s and p_g from p_h and p_y

Depending on the recording geometry, it may be more convenient to pick data in common-midpoint and common-offset, rather than in common-shot and common-geophone, coordinates. For instance, land data, for which $\Delta s = \Delta g$ (shot spacing equals geophone spacing), is most conveniently formed into common-shot and common-geophone gathers (see Figure 2a), so it is natural to slant-stack these gathers to find p_s and p_g. Marine data, on the other hand, is often recorded with the configuration $\Delta s = \Delta g/2$. Such data is most conveniently formed into common-offset and common-midpoint gathers (see Figure 2b), and these gathers can be slant-stacked and picked through a technique that is directly analogous to the previously described technique for determining p_s and p_g.

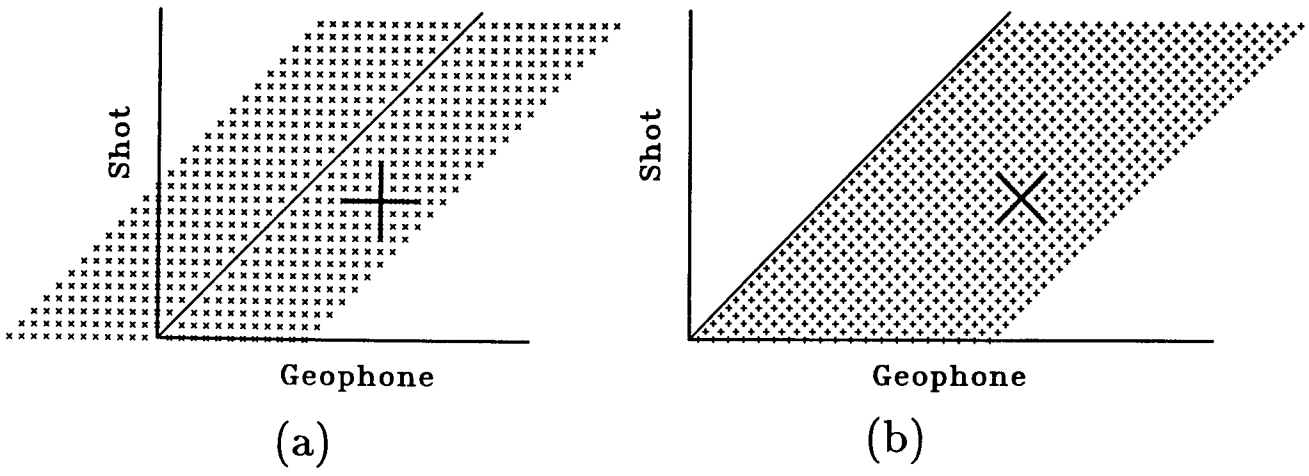

FIG. 2. Picking p_s and p_g versus picking p_y and p_h. Panel (a) shows the stacking chart (the geometry of the observation system) for a typical land experiment, where $\Delta s = \Delta g$. The dots represent seismic traces, and the heavy lines represent the gathers over which slant stacking takes place to determine p_s and p_g. Panel (b) shows the stacking chart for a typical marine experiment, where $\Delta s = \Delta g/2$. In such an experiment it is more convenient to choose gathers (shown by the heavy lines) which can be used to determine p_y and p_h.

In the notation used here, h, the half-offset, is defined by

$$h \equiv \tfrac{1}{2}(x_g - x_s), \tag{5}$$

while y, the midpoint, is defined by

$$y \equiv \tfrac{1}{2}(x_g + x_s), \tag{6}$$

where the shot and geophone positions are represented by x_s and x_g respectively. It is logical, then, to define p_h as the change in traveltime with respect to offset (with midpoint fixed), and p_y as the change in traveltime with respect to midpoint (with offset fixed).

Once p_y and p_h have been found from the slant-stacked midpoint and offset gathers, the corresponding values of p_s and p_g must be determined. The transformation is a simple one. Recall that

$$\begin{aligned} p_s &\equiv \frac{dt}{dx_s}, \qquad p_g \equiv \frac{dt}{dx_g}, \\ p_h &\equiv \frac{dt}{dh}, \qquad p_y \equiv \frac{dt}{dy}. \end{aligned} \tag{7}$$

Then

$$p_s = \frac{dt}{dx_s} = \frac{dt}{dy}\frac{dy}{dx_s} + \frac{dt}{dh}\frac{dh}{dx_s} = \tfrac{1}{2}(p_y - p_h), \tag{8}$$

and

$$p_g = \frac{dt}{dx_g} = \frac{dt}{dy}\frac{dy}{dx_g} + \frac{dt}{dh}\frac{dh}{dx_g} = \tfrac{1}{2}(p_y + p_h). \tag{9}$$

Thus, equations (8) and (9) show how to determine p_s and p_g, given p_y and p_h.

As will be discussed below, I have applied these picking techniques to a marine data set. This data was originally sampled with a geometry $\Delta s = \Delta g/4$, but I discarded every other shot profile, changing the geometry to $\Delta s = \Delta g/2$. Then I picked p_y and p_h from the slant-stack panels, and transformed to p_s and p_g.

Determining p_s and p_g from moveout-corrected data

It is often advantageous to apply a normal-moveout correction to the reflection seismic data before performing the slant stack (Riabinkin et al., 1962, p. 260). The normal-moveout correction reduces the apparent slope (ray parameter) of the far-offset data, thus reducing the risk of aliasing during the slant stack. In addition, the flattened data is more amenable to slant stacking, which is a process that assumes that traveltimes vary linearly, rather than hyperbolically, with horizontal position. The effects of the normal-moveout correction are removed when p_s, p_g, and t are calculated, so it doesn't matter whether the moveout-correction velocity used is accurate or not.

Suppose that all traces have been moveout corrected at a constant velocity v_0. Then the moveout-corrected traveltime t_{NMO} can be related to the old, uncorrected traveltime t by the formula

$$t = \sqrt{t_{\text{NMO}}^2 + \frac{4h^2}{v^2}}, \tag{10}$$

where h is the half-offset, as defined in equation (5). Then, by equation (10) and the definition of p_s,

$$p_s = \frac{dt}{dx_s} = \frac{1}{\sqrt{t_{\text{NMO}}^2 + \frac{4h^2}{v^2}}} \left(t_{\text{NMO}} \frac{dt_{\text{NMO}}}{dx_s} + \frac{4h}{v^2} \frac{dh}{dx_s} \right). \tag{11}$$

Let $p_{s\text{NMO}}$ be the measured change in moveout-corrected traveltime t_{NMO} with respect to shot position, and let $p_{g\text{NMO}}$ be the corresponding change with respect to geophone position. Then, by these definitions, equation (10), equation (11), and the definition of h,

$$p_s = \frac{1}{t} \left(t_{\text{NMO}}\, p_{s\text{NMO}} - \frac{2h}{v^2} \right). \tag{12}$$

Similarly, it can be shown that

$$p_g = \frac{1}{t} \left(t_{\text{NMO}}\, p_{g\text{NMO}} + \frac{2h}{v^2} \right). \tag{13}$$

Thus, equations (10), (12), and (13) show how t_{NMO}, $p_{s\text{NMO}}$, and $p_{g\text{NMO}}$, measured on moveout-corrected data, can be transformed to yield the parameters t, p_s, and p_g, just as if these parameters had been measured on data where the moveout correction was not applied. I used this transformation in determining the ray parameters for the marine data example to be discussed below; I chose a constant moveout-correction velocity of 1.6 km/sec.

Two-way slant stacks

Other investigators (Harlan and Burridge, 1983; Pan and Gardner, 1986) have proposed a so-called "two-way" slant stack that allows p_s and p_g to be determined simultaneously,

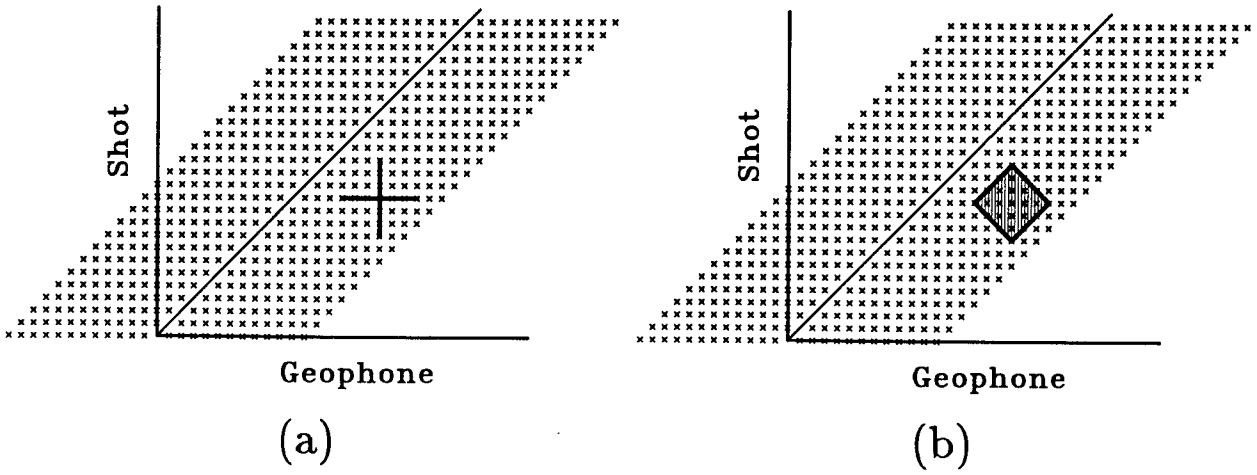

FIG. 3. Two-way slant stacking. Panel (a) shows a stacking chart from a typical land experiment, with heavy lines designating the gathers that are to be slant stacked to determine p_s and p_g (this is the same chart as in Figure 2a). Panel (b) shows the same stacking chart, but now a hatched square shows all the gathers that are to be included in a two-way slant stack. The two-way slant stack is more expensive than the conventional slant stack, but it is more resistant to noise, since more gathers are used.

without the need to cross-correlate between two separate slant-stack panels. It combines, in effect, equations (1) and (4), producing as output a three-dimensional function in p_s, p_g, and t:

$$r_{mn}(t) = \sum_{k=-n_{bh}}^{n_{bh}} \sum_{l=-n_{bh}}^{n_{bh}} u_{(i+k)(j+l)}(t + mk\Delta p\Delta s + nl\Delta p\Delta g). \tag{14}$$

Here m and n specify the values $p_s = m\Delta p$ and $p_g = n\Delta p$. This three-dimensional space can be searched for maxima and minima; the position of an individual peak directly gives p_s, p_g, and t.

An advantage of the two-way approach is that it makes use of more nearby traces in the slant stacking operation (see Figure 3); the signal/noise ratio is thus increased. Another advantage of this approach is that p_s and p_g are picked simultaneously, eliminating the need for a cross-correlation step. The main disadvantage is its expense.

INDIRECT PICKING METHODS

Sometimes it is more convenient to determine the reciprocal parameters x_s, x_g, p_s, p_g, and t from seismic data that has already been stacked. A primary reason might be the need to increase the signal/noise ratio. The main disadvantage of this approach is the implicit assumption that velocity only varies slowly horizontally. I have not tested this approach myself, but I shall discuss it here because of its potential advantages.

Determining p_s and p_g from t_0, p_{y_0}, and v

It is possible to determine p_s and p_g indirectly, from parameters that might not seem,

at first glance, to contain the necessary information. Suppose that data have been collected using an off-end (non-symmetrical) geometry. Furthermore, suppose that the data for interpretation consist of a stacked (unmigrated) section and the stacking velocity at each point. These data contain enough information to determine p_s and p_g.

A gather is formed from the traces centered around the trace at midpoint y_0 on the stacked section. Then a slant stack is performed on this gather, and peaks picked. If p_{y_0} is defined as the change in simulated zero-offset traveltime with respect to midpoint y, then the picking yields p_{y_0}, as well as the simulated zero-offset traveltime t_0, at midpoint y_0. (I use the word "simulated" to emphasize that these are not parameters taken from a true zero-offset section, but parameters taken from a stacked section, which is a simulated zero-offset section). It has been suggested (Will Gray, personal communication) that this picking step might be made semi-automated instead of fully automated, allowing an interpreter to eliminate spurious picks caused by multiple reflections or noise. The inclusion of an interpreter is feasible, since slant stacks are performed on a single stacked section, rather than (as in the methods previously described) on a large pre-stack data set.

Alternatively, $t_0(y)$ can be picked along a horizon. Then t_0 can be smoothed, and p_{y_0} determined explicitly from the formula $p_{y_0} = \Delta t_0/\Delta y$ (Glogovskii et al., 1979). If "bow ties" are present in the data, it may be difficult to pick the horizon $t_0(y)$. In such cases a preliminary migration can be applied to the data to regularize the horizon; the migrated horizon is picked, and then an inverse migration is applied to the picked horizon (Glogovskii et al., 1982). Such methods are considered to fall within the method of reciprocal points, although they are not related to CDR.

Three other parameters, besides t_0 and p_{y_0}, can be extracted from the stacked data set. One of these is y_0, the midpoint coordinate of the center trace in the slant-stacked gather. The second is v_0, the stacking velocity at midpoint y_0 and zero-offset traveltime t_0. The third, h_{avg}, represents a simulated half-offset. That is, it represents the offset at which the parameters are supposed to have been measured. For the present, it is convenient to assume that if h_{near} is the near half-offset (that is, half the distance from the source to the nearest receiver), and h_{far} is the far half-offset, then $h_{\text{avg}} = (h_{\text{near}} + h_{\text{far}})/2$. Note that h_{near} and h_{far} will probably vary with traveltime, depending on the muting scheme used. It is clear, now, why the original shooting geometry must be off-end: if the geophones are laid out symmetrically on both sides of the shot, then $h_{\text{avg}} = 0$, which leads to many complications, including the inability to perform tomographic velocity inversion.

From the five parameters t_0, p_{y_0}, h_{avg}, y_0, and v_0, it is possible to determine simulated values for the five reciprocal parameters x_s, x_g, t, p_s, and p_g; it may be helpful to smooth v_0 spatially before this determination is made (Glogovskii et al., 1979). The parameters x_s and x_g can be determined from y_0 and h_{avg}, if these latter two values follow the behavior of h and y in equations (5) and (6). Equations (5) and (6) are easily inverted to yield:

$$x_g = y_0 + h_{\text{avg}}, \qquad x_s = y_0 - h_{\text{avg}}. \tag{15}$$

The parameter t can be determined from the formula:

$$t = \sqrt{t_0^2 + \frac{4h_{\text{avg}}^2}{v_0^2}}. \tag{16}$$

Then

$$p_s = \frac{dt}{dx_s} = \frac{1}{t}\left(t_0\frac{dt_0}{dx_s} + 4\,\frac{h_{\text{avg}}}{v_0^2}\frac{dh_{\text{avg}}}{dx_s} - 4\,\frac{h_{\text{avg}}^2}{v_0^3}\frac{dv_0}{dx_s}\right). \tag{17}$$

Equation (16) is not strictly correct when velocity is allowed to vary spatially, so it is not clear whether the dv_0/dx_s term in equation (17) is meaningful. I will, however, retain terms of this type for the rest of the derivation; any readers who find them objectionable are free to set them equal to zero.

From an equation analogous to equation (5), $dh_{avg}/dx_s = -1/2$. And from the chain rule, the definition of p_{y_0}, and equation (6),

$$\frac{dt_0}{dx_s} = \frac{dt_0}{dy_0}\frac{dy_0}{dx_s} = \tfrac{1}{2}p_{y_0}. \tag{18}$$

Likewise,

$$\frac{dv_0}{dx_s} = \frac{dv_0}{dy_0}\frac{dy_0}{dx_s} = \tfrac{1}{2}\frac{dv_0}{dy_0}. \tag{19}$$

Then, from equations (16), (17), (18), and (19),

$$p_s = \frac{1}{2t}\left(t_0 p_{y_0} - 4\frac{h_{avg}}{v_0^2} - 4\frac{h_{avg}^2}{v_0^3}\frac{dv_0}{dy_0}\right), \tag{20}$$

and

$$p_g = \frac{1}{2t}\left(t_0 p_{y_0} + 4\frac{h_{avg}}{v_0^2} - 4\frac{h_{avg}^2}{v_0^3}\frac{dv_0}{dy_0}\right). \tag{21}$$

These results are similar to those given by Bandurin et al. (1982).

Thus equations (15), (16), (20) and (21) can be used to determine x_s, x_g, p_s, p_g, and t, once the parameters y_0, h_{avg}, p_{y_0}, t_0, and v_0 have been determined from the stacking velocity function, the stacked seismic data, and the recording geometry. An important advantage of this approach, over the direct picking methods previously described, is that more data is stacked together before the reciprocal parameters are chosen, thus making the reciprocal parameters more reliable. Another advantage, already mentioned above, is that this method involves picking data from a relatively small data set (a single stacked section), thus making it feasible for a human operator to prevent bad picks from being made. The main disadvantage to this approach seems to be its lack of spatial resolution: the data is stacked over an entire range of offsets. Another disadvantage is that in regions with crossing dipping reflectors, the stacking velocity v_0 is, in theory, multivalued. This method, with its advantages and disadvantages, is being used in practice (Kopilevich et al., 1986).

There are a couple of useful tricks associated with this method. Although h_{avg} was defined previously to lie half-way between h_{near} and h_{far}, it is actually possible to use an arbitrary value of h_{avg} in the range $h_{near} \le h_{avg} \le h_{far}$; despite appearances, the reciprocal parameters are only somewhat sensitive to the value of h_{avg}. In fact, several sets of reciprocal parameters can be picked at a single traveltime and midpoint, by plugging in different values of h_{avg} into equations (15), (16), (20) and (21); this use of multiple h_{avg} values can help increase the stability of the inversion (Glogovskii et al., 1979).

Windowing over offset

One way to retain the advantages of the indirect method (the reduction of noise by stacking more data), while increasing the resolution, is to perform the preliminary stacking and velocity analysis over a narrower range of h (half-offset) values. The transformation

equations (equations (15), (16), (20), and (21)) remain valid; the only change is that h_{avg} now represents the average offset over the offset window.

This idea can be combined with the two-way stack approach. A gather of traces, centered around a particular midpoint and offset, is formed. Then a slant stack over the midpoint coordinate is carried out simultaneously with a velocity analysis stack (normal-moveout correction at various velocities, plus stack) over the offset coordinate (Kostov and Biondi, 1987). The result is a three-dimensional data volume with coordinates v_0, p_{y_0}, and t (Urupov and Levin, 1985, pp. 172–174). Peaks can be picked from this volume, and the reciprocal parameters found according to the transformation equations.

CORRELATED CDR

In the Soviet Union, a method known as Correlated CDR has recently been developed (Zavalishin, 1981). It is, in some ways, a hybrid between indirect and direct methods for determining p_s and p_g. In this method it is necessary only to know an approximate velocity, rather than an exact stacking velocity. Thus, it is better suited than indirect methods to regions with crossing dipping reflectors, since in such regions the stacking velocity is, in theory, multi-valued. I will not describe the Correlated CDR method here, since its description is rather lengthy, and the main reference is already available in an English translation.

CDR MIGRATION, VELOCITY ANALYSIS, AND IMAGING

Once the reciprocal parameters, x_s, x_g, p_s, p_g, and t, have been determined, they can be used to construct migrated sections. An effective velocity can be determined for each set of parameters as well; this effective velocity is used in the migration (imaging) process and in velocity filtering.

CDR constant-velocity depth migration

The reciprocal parameters can be used to produce constant-velocity migrated sections. The only difficulty is deciding which information to use. For instance, suppose the five reciprocal parameters, x_s, x_g, p_s, p_g, and t, are known for a particular event; each of these parameters has some uncertainty associated with it. Suppose, in addition, that an *a priori* constant velocity is known (or guessed) for the medium. The problem of determining the location and dip of the reflecting segment that generated the reflection event is now overdetermined. As will be seen below, the five reciprocal parameters are, by themselves, sufficient to determine the effective velocity of the medium, as well as the position and dip of the reflector; thus, the *a priori* constant velocity adds redundant information.

The five reciprocal parameters are not all known to the same degree of accuracy. I consider the parameters x_s and x_g to be accurately known; they represent the physical position of the shot and geophone, so they are known within the precision of the land survey (others might argue that they are only known within an accuracy given by the spread lengths $n_{\text{base}}\Delta s$ and $n_{\text{base}}\Delta g$). I also find it reasonable to assume that the least accurately known parameters are the ray parameters p_s and p_g. The parameter t, then, I consider to be of intermediate accuracy (the main errors in determining t are caused by the length and phase characteristics of the source wavelet).

Imaging the reflecting segment

If the shot and geophone positions, x_s and x_g, are known, as are the *a priori* velocity v and the traveltime t, then the reflecting segment must lie at a point (y_R, z_R), somewhere along the ellipse described by the formula:

$$z_R^2 = \left(1 - \frac{4h^2}{v^2t^2}\right)\left(\frac{v^2t^2}{4} - (y_R - y)^2\right), \tag{22}$$

where h and y are defined according to equations (5) and (6). This ellipse is known as an "aplanatic surface" (Gardner, 1949).

Note that equation (22) was determined without any recourse to the ray parameters p_s and p_g. These two parameters were intentionally excluded, since they are considered less reliable. They are used, however, to find the specific point on the ellipse where the reflecting segment lies. This reflecting segment is assumed to have a dip ϕ, which can be determined by means of p_s and p_g. In a constant-velocity medium, the ray parameter p corresponds to a ray traveling at an angle θ to the vertical, with the correspondence given by the equation $\sin\theta = vp$. Thus, we can speak of the shot ray traveling at an angle θ_s, and the geophone ray traveling at an angle θ_g, with these angles given according to the formulas

$$\begin{aligned} \sin\theta_s &= vp_s, \\ \sin\theta_g &= vp_g. \end{aligned} \tag{23}$$

If the reflecting segment has a dip of angle ϕ, and Snell's law is assumed to hold, so that the angle of incidence of the shot ray equals the angle of incidence of the geophone ray, then it can be shown, after some algebra, that

$$\tan\phi = \frac{v(p_s + p_g)}{\sqrt{1 - v^2p_s^2} + \sqrt{1 - v^2p_g^2}}. \tag{24}$$

Once the dip angle ϕ is determined, it is possible to locate, on the ellipse described by equation (22), the point where a tangent line has the identical dip angle ϕ. The reflecting segment must lie at this point. Equation (22) can be differentiated with respect to y_R, and the substitution $dz_R/dy_R = -\tan\phi$ made (the minus sign results because in this system of coordinates, z_R increases with depth); solving for y_R yields the formula

$$y_R = y + \frac{\frac{vt}{2}\tan\phi}{\sqrt{1 - \frac{4h^2}{v^2t^2} + \tan^2\phi}}, \tag{25}$$

which gives the horizontal position, y_R, of the reflector, in terms of the five reciprocal parameters and the *a priori* velocity. Substituting this equation into equation (22) yields

$$z_R = \frac{\frac{vt}{2}\left(1 - \frac{4h^2}{v^2t^2}\right)}{\sqrt{1 - \frac{4h^2}{v^2t^2} + \tan^2\phi}}, \tag{26}$$

which gives the depth of the reflector.

Thus, given the five reciprocal parameters and an *a priori* velocity, it is possible to use equations (24), (25), and (26) to find a dipping line, with dip angle ϕ and position (y_R, z_R), corresponding to the dipping reflector that must have originally generated the event. This dipping line (or dip bar) can be plotted, along with other dipping lines corresponding to other sets of reciprocal parameters, to give what is, in effect, a constant-velocity migrated depth section.

The length of the reflecting segment

In order to construct a reasonable migrated depth section, it is necessary to know how long to draw the dipping lines that are supposed to represent the dipping reflectors. Typically the length of the plotted dip bar is proportional to the resolution length of the reflecting segment; here "resolution length" is understood to mean the shortest distance, along the reflector, for which a change in reflector characteristics can be resolved. This length can be estimated from the size of the Fresnel zone (Zavalishin, 1975); such estimates show the resolution length to be proportional to the square root of depth. Other estimates of this length are based on the uncertainty in the ray parameter p (Kozlov et al., 1975); these estimates show the resolution length to be directly proportional to depth. Depending on the dominant wavelength of the source wavelet, the width of the array over which slant stacking is performed, and the depth of the reflector, one or the other of these estimates may give the limiting resolution length (Phinney and Jurdy, 1979).

The question of reflector resolution is of interest to those who interpret the results of CDR migration, but it is not necessarily relevant to the problem of tomographic velocity estimation. The estimated velocity structure is much more poorly resolved than are the reflectors; thus, it is not really important, for velocity analysis, whether the reflector resolution varies directly or with the square root of depth. The plots in this chapter were plotted with dip bars whose length varies as the square root of depth. However, the multiplicative constant used to determine the absolute length of the dip bars was chosen with the to make reasonable-looking plots, rather than to show the true resolution length.

CDR velocity analysis

The five reciprocal parameters, x_s, x_g, p_s, p_g, and t, are all that is needed to determine the velocity in the medium, if that velocity is assumed to be constant. The formula for determining this velocity is well-known in the Soviet Union; it is independent of the dip or curvature of the reflecting horizon (Puzyrev, 1979, p. 222; Goldin, 1984, p. 27). This formula was independently and simultaneously developed in about 1945 by three Soviet scientists: N.N. Puzyrev, Iu.V. Riznichenko, and V.N Rudnev (Urupov and Levin, 1985, p. 147):

$$v_{\text{CDR}}^2 = \frac{1 - \frac{h}{t}(p_s - p_g)}{(p_s - p_g)\frac{t}{4h} + p_s p_g}, \tag{27}$$

where v_{CDR} is defined to be the velocity determined through use of the reciprocal parameters, and h is as defined in equation (5). Note that as h approaches zero, this equation becomes more sensitive to errors in p_s and p_g.

The value v_{CDR} is an averaged velocity. It is analogous to average velocity, which is

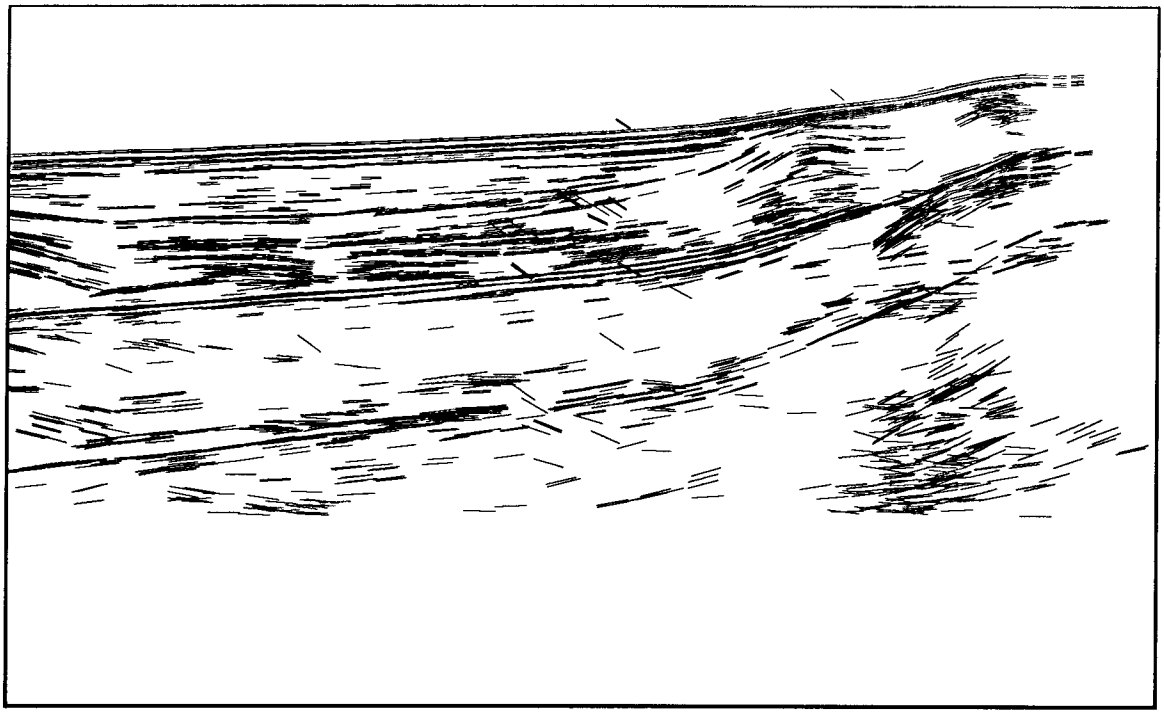

FIG. 4. CDR migrated depth section. Marine data from offshore southern California (courtesy of British Petroleum) were picked, and the resulting reciprocal parameters were depth migrated (as described in the text) at a constant velocity of 1.48 km/sec (water velocity). Note that while the water-bottom reflection and multiples are well focused, the other events are rather fuzzy.

defined according to the formula

$$v_{\text{avg}}(t) \equiv \frac{z}{\int_0^z 1/v(z')dz'}, \tag{28}$$

and root-mean-square velocity, which is defined according to the formula

$$v_{\text{rms}}{}^2(t) \equiv \frac{\int_0^z v(z')dz'}{\int_0^z 1/v(z')dz'}, \tag{29}$$

where $v(z)$ is the interval velocity. The value v_{CDR} is known, in Soviet seismological terminology, as a "differential effective parameter" (Puzyrev, 1979). For flat layers, v_{CDR} approaches v_{rms} as offset h approaches zero (Urupov and Levin, 1985, p. 103). As will be seen below, v_{CDR} is used for velocity filtering and for producing plots. It is not, however, directly used in the process of tomographic velocity analysis.

CDR display techniques

One of the most interesting aspects of the method of Controlled Directional Reception is the speed and flexibility it allows in plotting the picked data. CDR data are quickly migrated, and they contain information not found in other representations of seismic data:

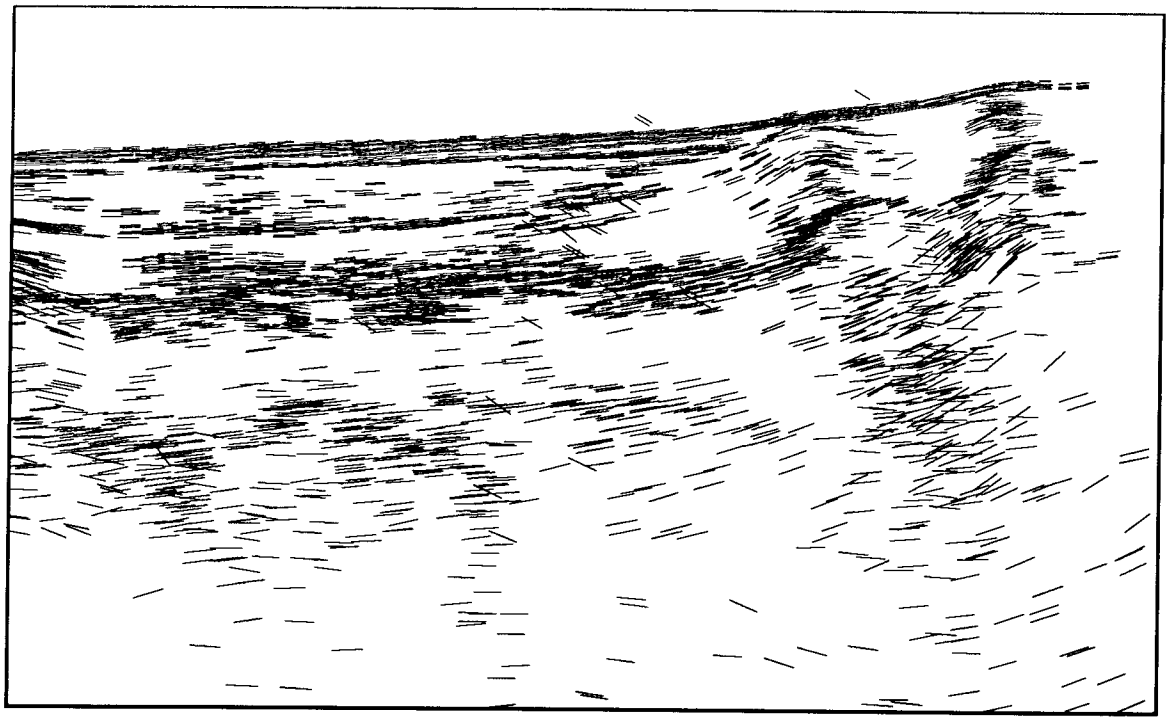

FIG. 5. CDR depth-migrated section ($v = v_{\text{CDR}}$). The same picked parameters are used as were used in producing Figure 4, but each dipping line is migrated at its own CDR velocity v_{CDR} (see text), rather than at a constant migration velocity. Because of noise-induced variations in v_{CDR}, the reflectors are fuzzy.

for instance, a velocity, v_{CDR}, can be associated with each dip bar. Examples of this flexibility in plotting will be shown below; the examples are based on picked marine seismic data (the data, from offshore southern California, are provided courtesy of British Petroleum). Strong water-bottom multiples are evident in all the examples.

CDR depth migration

Equations (24), (25), and (26), given previously, provide all the information necessary for constructing a constant-velocity depth-migrated section. Such a section is illustrated in Figure 4, which was constructed assuming a constant velocity $v = 1.48$ km/sec (water velocity). Note that the water-bottom reflection and the water-bottom multiples are well focused; other reflectors appear fuzzier.

A different type of depth migration is possible when the velocity $v = v(x, z)$ is assumed to be known *a priori*. Then ray-tracing techniques can be used, for each set of reciprocal parameters, to determine the position of the associated reflecting segment. The difficulty is that, as in a previous section, the problem is overdetermined.

Taking advantage of v_{CDR}

The CDR migration velocity v_{CDR} is used to produce certain types of plots. It has to be used carefully, however; v_{CDR} is not stable—it can vary a great deal owing to variations in p_s and p_g, especially if the half-offset h is small compared to the depth of the reflector.

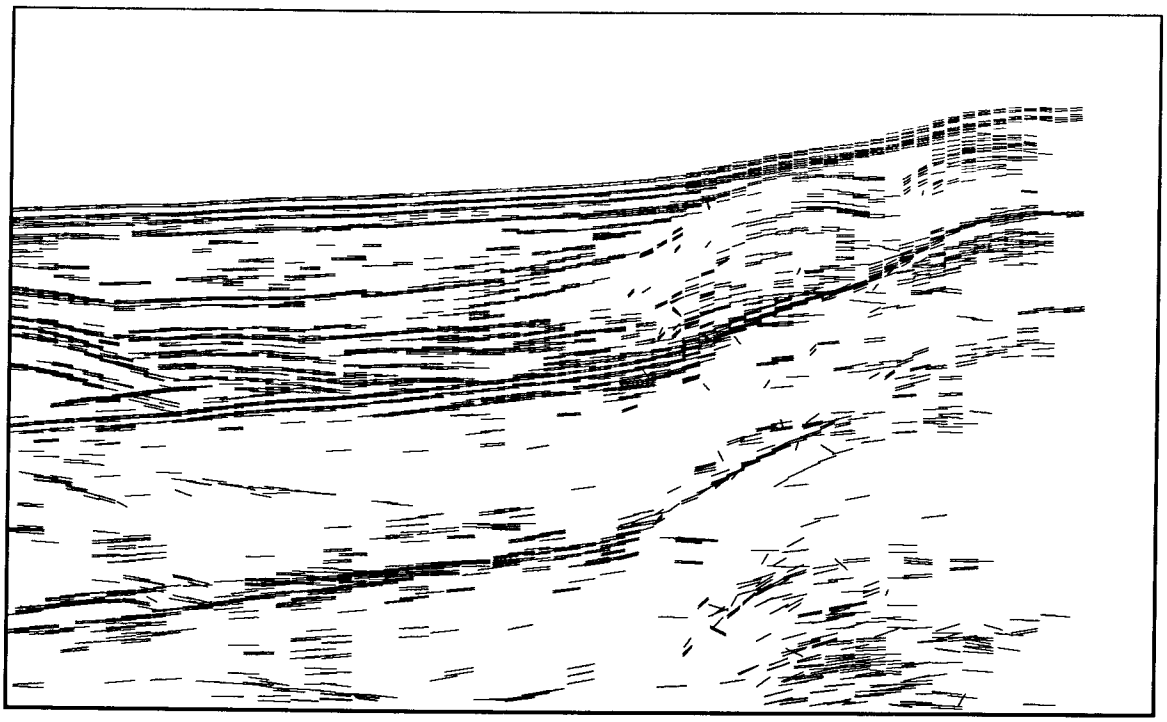

FIG. 6. CDR simulated stacked section ($v = v_{\text{CDR}}$). Picked parameters from the British Petroleum marine data set are used. Only a normal-moveout correction has been applied to the picked parameters. This normal-moveout correction is based on the value of the CDR velocity v_{CDR} associated with each dip bar. The reflectors in this figure are much less fuzzy than in Figure 5; the main reason is that the dip bars are plotted with a vertical axis that represents time rather than depth.

For instance, a misapplication of v_{CDR} would be to use it to produce a depth-migrated plot. In theory, of course, v_{CDR} can be used in place of the *a priori* velocity v in equations (24), (25), and (26), to produce a depth-migrated plot where each dip bar has been located according to its associated CDR velocity v_{CDR}. The problem, as seen in Figure 5, is that the variations in v_{CDR} translate into variations in z_{R}, the migrated depth, in the final plot. These variations in depth lead to a loss in coherency of the reflectors.

There are other types of plots, however, where using v_{CDR} is entirely appropriate. The main advantage of using v_{CDR} in producing plots, as will be seen below, is that well-focused plots, including time-migrated sections, can be produced without the need to perform a preliminary velocity analysis. If v_{CDR} is properly used, then the effect is as if a separate velocity analysis were performed for every reflection event.

CDR simulated stacking

An example of the appropriate use of v_{CDR} is in producing a simulated stacked section. A simulated stacked section is supposed to reproduce the effects of applying a normal-moveout correction and stacking unpicked data. The simulated stacked section is produced by determining, for each set of picked reciprocal parameters, the plotting parameters p_{y_0} (the apparent dip of the reflecting segment), y_{R} (the midpoint location of the reflecting segment), and t_{R} (the moveout-corrected traveltime to the reflecting segment). These plotting

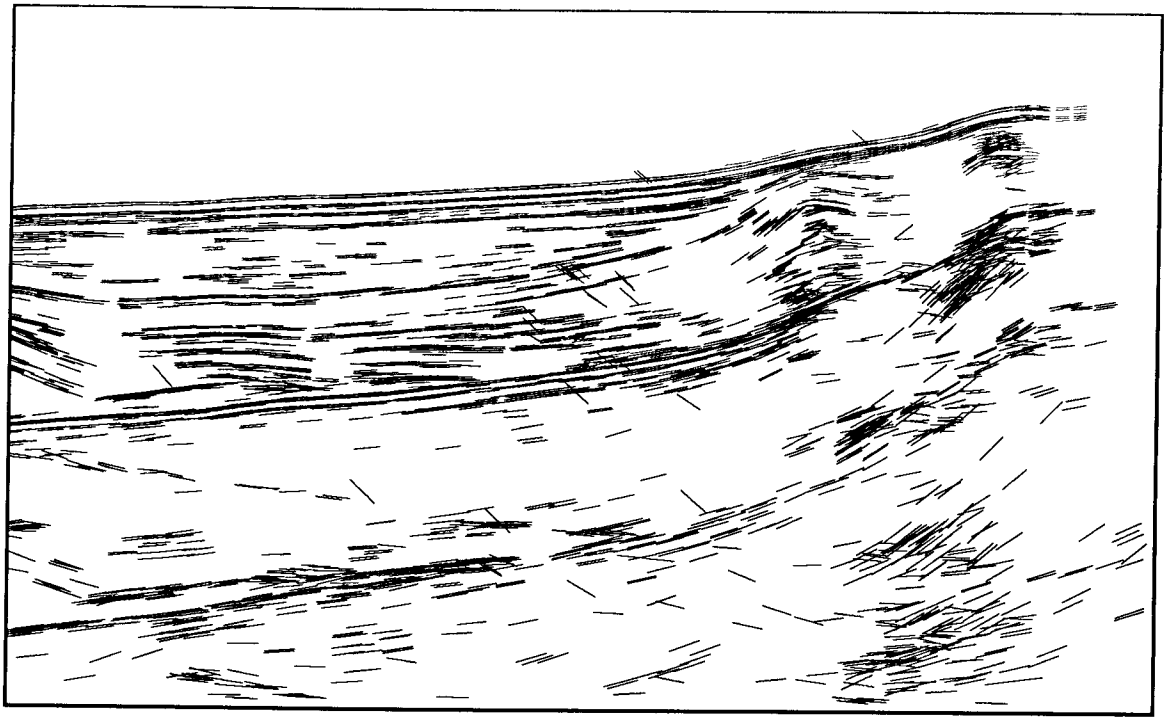

FIG. 7. CDR migrated time section ($v = v_{\text{CDR}}$). The picked British Petroleum marine data have been time migrated, with each dip bar migrated according to its associated CDR velocity v_{CDR}. The reflectors are much less fuzzy than in the depth migration in Figure 5; the main reason is that the vertical axis in the plot now represents time rather than depth, so that fluctuations in v_{CDR} induce only small vertical fluctuations in the positions of the dip bars.

parameters are found according to the formulas

$$y_{\text{R}} = y, \tag{30}$$

$$t_{\text{R}} = \sqrt{t^2 - \frac{4h^2}{v_{\text{CDR}}^2}}, \tag{31}$$

and

$$p_{\text{y0}} = \frac{1}{t_{\text{R}}}\left[t(p_{\text{s}} + p_{\text{g}}) - \frac{4h}{v_{\text{CDR}}^2}\right], \tag{32}$$

where h is the half-offset, defined in equation (5), and y is the midpoint, defined in equation (6). The derivation of equation (30) is obvious (the midpoint is unchanged after a simple normal-moveout correction), and equations (31) and (32) are derived in a fashion analogous to the derivation of equations (16) and (20). Figure 6 shows the result of plotting such a simulated stacked section. The jitter is much less obvious than in Figure 5; this is a consequence of remaining in the traveltime domain rather than converting to depth.

CDR time migration

It has been seen that the CDR velocity v_{CDR} can be successfully used to image data, as long as a time-to-depth conversion is not made. This result suggests that time migration

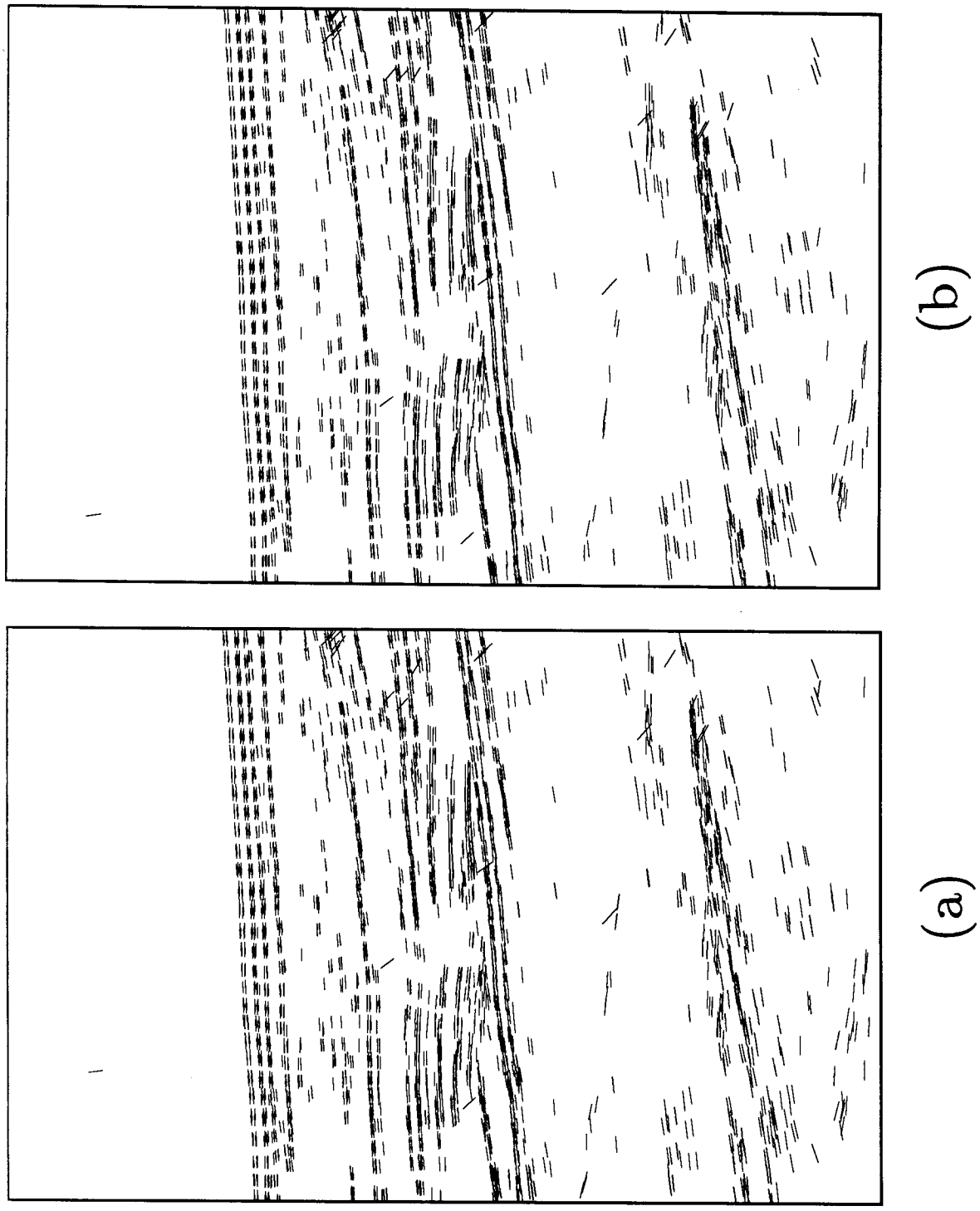

FIG. 8. Stereo pair. Panel (b) is an expanded portion of Figure 7 (a CDR time-migrated section). Panel (a) is similar, except that each dip bar has been shifted to the right in proportion to the associated value of v_{CDR}. The result is a stereo plot. If viewed with a stereo viewer (or with crossed eyes), an illusion of depth is created, with v_{CDR} as the third dimension. The water-bottom reflection and its multiples all have low velocities, causing them to stand out from the higher-velocity primary reflections.

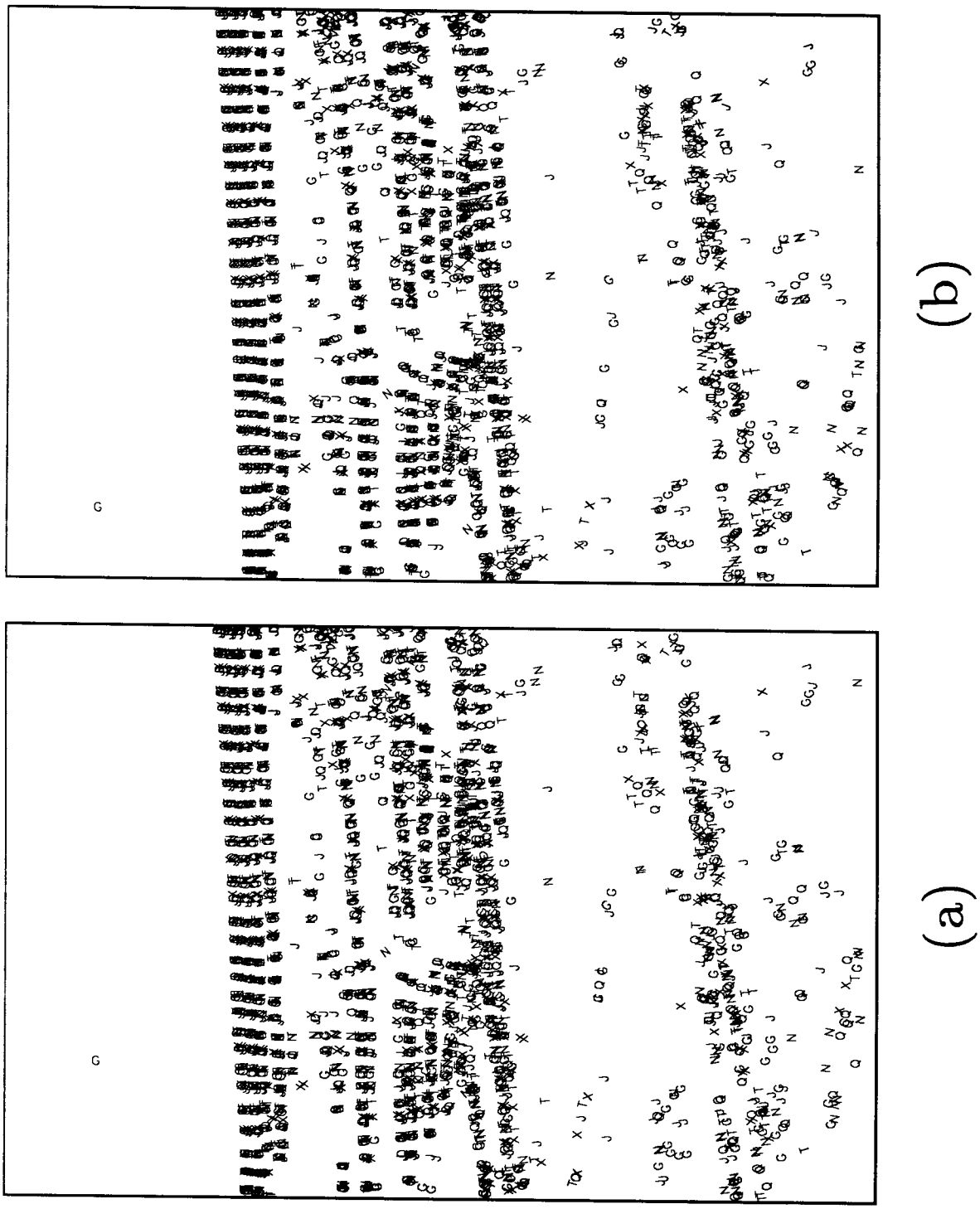

FIG. 9. A more complicated stereo plot. This figure is identical to Figure 8, except that the dip bars have been replaced by letters of the alphabet. Letters close to A represent dip bars recorded at near offsets (x_s near x_g); letters closer to Z represent dip bars recorded at far offsets.

might be more successful than depth migration in taking advantage of $v_{\rm CDR}$. To carry out such a time migration, equations (24), (25), and (26) are used (with $v_{\rm CDR}$ instead of an *a priori* v) to determine the quantities $\tan\phi$, $y_{\rm R}$, and $z_{\rm R}$. Then a simple depth-to-time conversion converts $z_{\rm R}$ into the time domain:

$$t_{\rm R} = \frac{2z_{\rm R}}{v_{\rm CDR}}; \tag{33}$$

a similar formula converts $\tan\phi$:

$$p_{y_0} = \frac{2}{v_{\rm CDR}} \tan\phi. \tag{34}$$

The plotting parameters $y_{\rm R}$, $t_{\rm R}$, and p_{y_0} tell where, and with what apparent dip, the time-migrated reflector segment should be plotted. An example of such a time migration is shown in Figure 7.

Stereo velocity displays

The CDR velocity $v_{\rm CDR}$ can serve as extra information for the interpreter, if a way can be found to display it. One interesting technique is to display $v_{\rm CDR}$ in the third dimension, letting depth into the plotted section be proportional to the measured CDR velocity. Such a display is made by means of simple stereo techniques. Two images are plotted: one is plotted normally, and the other is plotted with each dip bar shifted to the right (or left) by an amount proportional to the associated value of $v_{\rm CDR}$. Such a stereo plot (time-migrated as in Figure 7) is shown in Figure 8. Note that the water-bottom multiples, all of which have a $v_{\rm CDR}$ of about 1.5 km/sec, stand out clearly from the higher-velocity primary reflections.

Even more information can be put onto a single plot. For instance, it may be interesting to see how $v_{\rm CDR}$ varies with offset. The stereo display in Figure 9 contains such information; it is identical to Figure 8, except that each dip bar has been replaced by a letter of the alphabet. Earlier letters (A, B, C, and so on) replace near-offset dip bars (dip bars whose reciprocal parameters were measured for $x_{\rm s}$ close to $x_{\rm g}$), while later letters (R, S, T, and so on) replace far-offset dip bars. Such displays should be used with caution; they may overwhelm rather than aid the interpreter.

PICKING REAL DATA

The previous figures were produced using picked data from a British Petroleum seismic survey off Southern California. These data served as a test for the CDR picking program that I developed.

Comparison of picked data to the original section

It is useful to compare how well the picked marine data correspond to the original, unpicked data. This is best done by converting the CDR simulated stacked section (Figure 6) from a line drawing to a conventional plot, as in Figure 10 (to make this plot, picked amplitude information was used in addition to the five reciprocal parameters). This section can be compared to a near-offset section from the unpicked data (Figure 11). It is seen that the picking process was successful in detecting most major events, without picking too many spurious events (noise). The traces were gained by a factor of $t^{1.5}$ before picking.

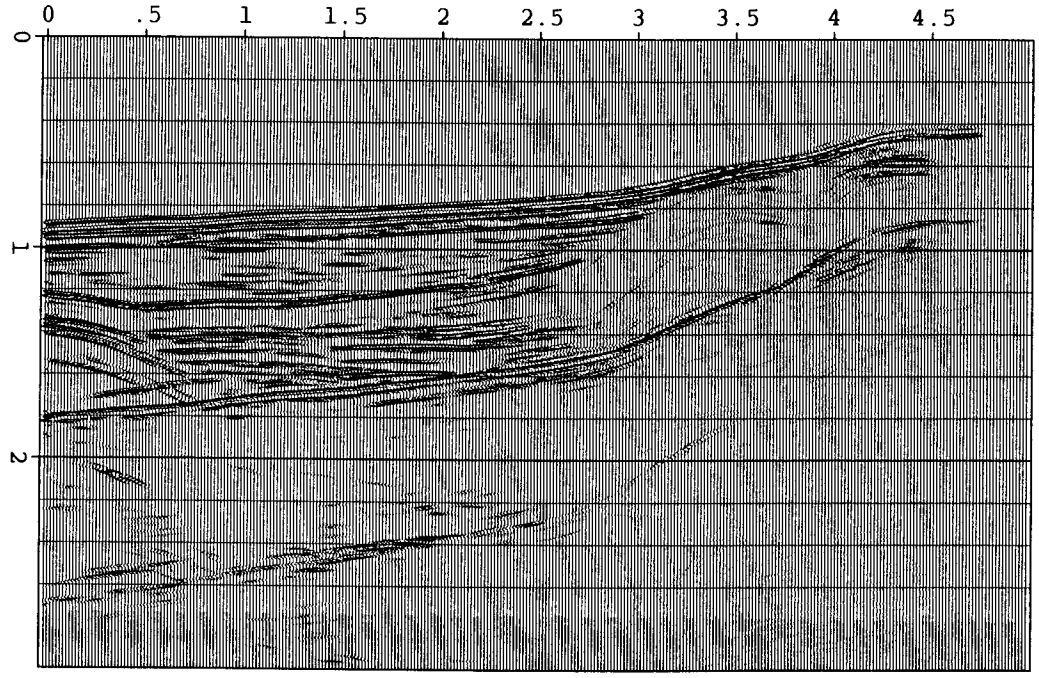

FIG. 10. CDR simulated stacked section (conventional plot). This, like Figure 6, is a simulated stacked section, but the dip bars have been plotted in a more conventional format.

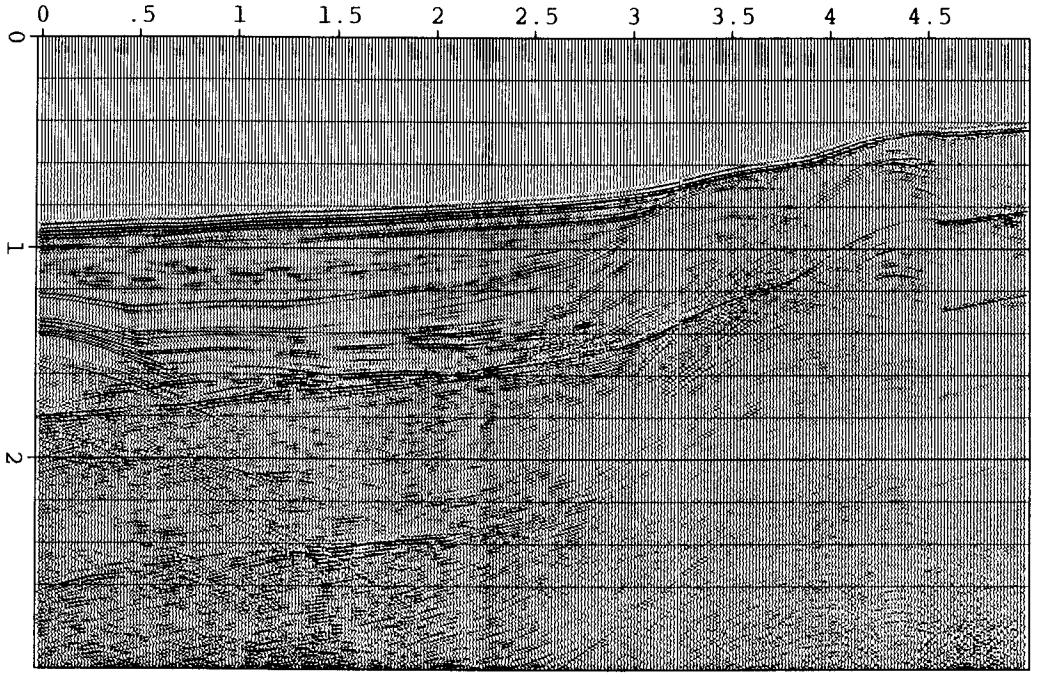

FIG. 11. Conventional plot of near-offset seismic data. This figure shows the British Petroleum marine data before picking. A comparison with Figure 10 shows the accuracy of the CDR picking procedure.

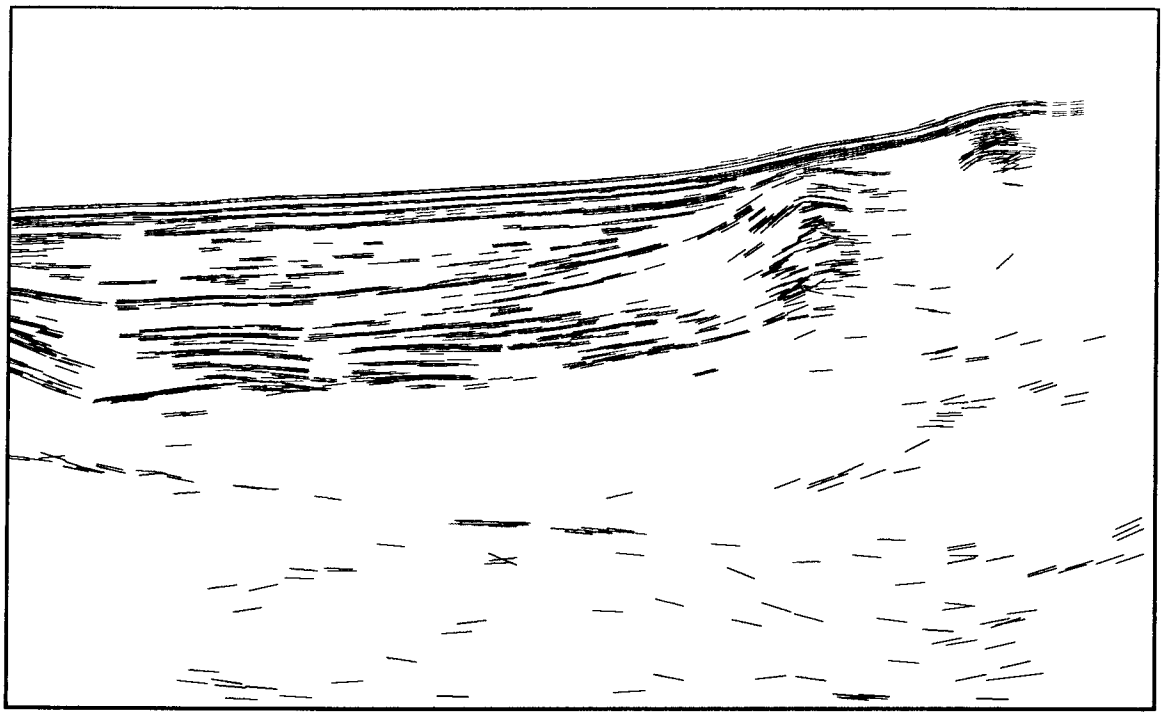

FIG. 12. Filtered time-migrated section. These are the same data as in Figure 7, except that undesirable events (such as multiple reflections) have been filtered out on the basis of amplitude, CDR velocity, and dip. Note the deep dipping reflector that is now visible. Note also that the second water-bottom multiple has not been completely eliminated.

Velocity and amplitude filtering

CDR tomographic inversion is not able to deal intelligently with multiples. It is desirable, then, to filter out multiple reflections, and other noise as well, before beginning the inversion process. The easiest way to filter out multiple reflections from CDR data is on the basis of CDR velocity, v_{CDR}; other spurious data can likewise be filtered out on this basis (Zavalishin et al., 1982). This filtering process requires some assistance from an interpreter, who must specify which values of v_{CDR} are acceptable at a given traveltime and midpoint. The main difficulty with velocity filtering is that when depth is large with respect to offset, the value v_{CDR} is not accurately determined, and owing to this inaccuracy, spurious events, such as multiples, can appear to have "reasonable" velocities.

Another useful technique for dealing with spurious data is amplitude filtering. When the five reciprocal parameters are picked, it is usual to pick amplitude as well; an anomalously low amplitude suggests that the associated reflection event is weak or spurious. Such low-amplitude events can usually be rejected.

Figure 12 shows a time-migrated section, analogous to Figure 7, where many undesirable events have been filtered out on the basis of their anomalous velocity, low amplitude, or anomalous dip.

CONCLUSIONS

The CDR method is an interesting and useful technique for converting a large seismic data set into a relatively small number of picked parameters. These picked parameters can be used to produce sections migrated in depth and time. Each set of picked parameters has an associated velocity; this velocity can be used in the migration process.

Most of the material in this chapter is based on ideas developed over the last several decades in the U.S.S.R. It is likely that most or all of the equations in this chapter have been published at one time or another in the geophysical literature, although I have not been able to locate references for many of them. As far as I have been able to determine, however, the stereo display of dip bars has not been previously tried.

ACKNOWLEDGMENTS

The real-data examples in this paper would not have been possible without the work of Paul Fowler, who spent a great deal of time reformatting and editing the British Petroleum marine data set, and who made it available in a standard format. I would like to thank him now for sharing his carefully prepared data with me.

I studied certain aspects of the CDR method during a 9-month visit to Moscow in 1983–84; this visit was sponsored by the International Research and Exchange Board. I would like to thank all the researchers at the Gubkin Oil and Gas Institute in Moscow who gave their advice on my halting attempts to understand the CDR method; I especially thank Boris Zavalishin and Yevgenii Varov.

In addition, I would like to thank Will Gray, Bill Harlan, Jeff Thorson, Rick Ottolini, Paul Fowler, and Biondo Biondi for helpful discussions.

REFERENCES

Bandurin, S.I., Bogoliubskii, A.D., Kopilevich, E.A., Sorin, V.Ia., and Ianovskii, A.K., 1982, Software for constructing seismic depth sections from CDP data on a medium-class ES computer: Exploration Geophysics, **95**, 31–39 (in Russian: Бандурин С.И., Боголюбский А.Д., Копилевич Е.А., Сорин В.Я., Яновский А.К., 1982, Математическое обеспечение построения глубинных сейсмических разрезов по данным МОГТ на ЭВМ ЕС среднего класса: Разведочная геофизика, вып. 95, с. 31–39).

Gardner, L.W., 1949, Seismograph determination of salt-dome boundary using well detector deep on dome flank: Geophysics, **14**, 29–38.

Glogovskii, V.M., Meshbei, V.I., and Tseitlin, M.I., 1979, An algorithm for determining parameters of layered media using the reciprocal points of reflection seismic travel time curves: Exploration Geophysics, **86**, 30–42 (in Russian: Глоговский В.М., Мешбей В.И., Цейтлин М.И., 1979, Алгоритм определения параметров слоистой среды по взаимным точкам годографов отраженных волн: Разведочная геофизика, вып. 86, с. 30–42).

Glogovskii, V., Meshbei, V., Tseitlin, M., and Langman, S., 1982, Kinematic-dynamic transformation of seismic traces for the determination of the velocity and depth structure of a medium, *in* Collection of reports to the second scientific seminar of COMECON countries on oil geophysics: Moscow, vol. 1, 327–331 (in Russian: Глоговский В., Мешбей В., Цейтлин М., Лангман С., 1982, Кинематико-динамическое преобразование сейсмической записи для определения скоростного и глубинного строения среды: в сб.: Сборник докладов второго научного семинара стран-членов СЭВ по нефтяной геофизике, Москва, т. 1, с. 327–331).

Goldin, S.V., 1986, Seismic traveltime inversion: Tulsa, Society of Exploration Geophysicists.

Harlan, W., and Burridge, R., 1983, A tomographic velocity inversion for unstacked data: SEP–37, 1–7.

Hermont, A.J., 1979, Letter to the Editor, re: Seismic controllable directional reception as practiced in the U.S.S.R.: Geophysics, **44**, 1601–1602.

Kong, S.M., Phinney, R.A., and Chowdhury, K.R., 1985, A nonlinear signal detector for enhancement of noisy seismic record sections: Geophysics, **50**, 539–550.

Kopilevich, E.A., Sharapova, E.S., Bogoliubskii, A.D., Brodskii, A.Ia., Parasyna, V.S., and Nediliuk, L.P., 1986, The effectiveness of implementing a programming-methodological complex for the automatic interpretation of reflection seismic data on an ES computer: Exploration Geophysics, **104**, 45–52 (in Russian: Копилевич Е.А., Шарапова Е.С., Боголюбский А.Д., Бродский А.Я., Парасына В.С., Недилюк Л.П., 1986, Эффективность внедрения программно-методического комплекса автоматизированной интерпретации данных МОГТ на ЕС ЭВМ: Разведочная геофизика, вып. 104, с. 45–52).

Kostov, C., and Biondi, B., 1987, Improved resolution of slant stacks using beam stacks: SEP–51 (this volume).

Kozlov, E.A., Mushin, I.A., and Tsyplakova, N.M., 1975, Construction of dynamic depth sections using the principles of the method of controlled directional reception: Applied Geophysics, **79**, 3–17 (in Russian: Козлов Е.А., Мушин И.А., Цыплакова Н.М., 1975, Построение динамических глубинных разрезов с использованием принципов метода регулируемого направленного приема: Прикладная геофизика, вып. 79, с. 3–17).

Pan, N.D., and Gardner, G.H.F., 1986, The p, q algorithm for seismic data analysis: 56th Annual International SEG Meeting, Houston, Texas.

Phinney, R.A., and Jurdy, D.M., 1979, Seismic imaging of deep crust: Geophysics, **44**, 1637–1660.

Puzyrev, N.N., 1979, Time fields of reflected waves and the method of effective parameters: Novosibirsk, Nauka (in Russian: Пузырев Н.Н., 1979, Временные поля отраженных волн и метод эффективных параметров: Новосибирск, Наука).

Rapoport, M.B., 1977, Determination of wave parameters through the CDR summation of seismic traces, *in* Riabinkin, L.A., Ed., Digital processing of reflection seismic data: Transactions of the Gubkin Institute of Petrochemical and Gas Production (Moscow), **120**, 17–22 (in Russian: Рапопорт М.Б., 1977, Определение параметров волн при суммировании сейсмических записей по МРНП: в сб.: Цифровая обработка данных сейсморазведки: Труды МИНХ и ГП, вып. 120., с. 17–22).

Riabinkin, L.A., Napalkov, Iu.V., Znamenskii, V.V., Voskresenskii, Iu.N., and Rapoport, M.B., 1962, Theory and practice of the CDR seismic method: Transactions of the Gubkin Institute of Petrochemical and Gas Production (Moscow), **39** (in Russian: Рябинкин Л.А., Напалков Ю.В., Знаменский В.В., Воскресенский Ю.Н., Рапопорт М.Б., 1962, Теория и практика сейсмического метода РНП: Труды МИНХ и ГП, вып. 39).

Rieber, F., 1936, A new reflection system with controlled directional sensitivity: Geophysics, **1**, 97–106.

Schultz, P.S., and Claerbout, J.F., 1978, Velocity estimation and downward continuation by wavefront synthesis: Geophysics, **43**, 691–714.

Stoffa, P.L., Buhl, P., Diebold, J.B., and Wenzel, F., 1981, Direct mapping of seismic data to the domain of intercept time and ray parameter—a plane wave decomposition: Geophysics, **46**, 255–267.

Urupov, A.K., and Levin, A.N., 1985, The determination and interpretation of velocities in reflection seismology: Moscow, Nedra (in Russian: Урупов А.К., Лёвин А.Н., 1985, Определение и интерпретация скоростей в методе отраженных волн: Москва, Недра).

Zavalishin, B.R., 1975, On the dimensions of the portion of a boundary which forms a reflected wave: Applied Geophysics, **77**, 67–74 (in Russian: Завалишин Б.Р., 1975, О размерах участка границы формирующего отраженную волну: Прикладная геофизика, вып. 77, с. 67–74); see SEP–28, 345–353 for an English translation.

Zavalishin, B.R., 1981, Perfection of methods for constructing seismic images using controlled direct reception: Soviet Geology and Geophysics, no. 10, 98–104 (English translation of: Завалишин, Б.Р., 1981, Совершенствование приемов построения сейсмических изображений по методу РНП: Геология и геофизика, № 10, с. 114–122); see SEP–30, 63–75 for alternate English translation.

Zavalishin, B.R., Voskresenskii, Iu.N., and Konopliantsev, M.A., 1982, Interpretational selection of waves for the faster construction of CDR dynamic depth sections: Applied Geophysics, **102**, 37–48 (in Russian: Завалишин Б.Р., Воскресенский Ю.Н., Коноплянцев М.А., 1982, Интерпретационый отбор волн при ускоренном построении динамических глубинных разрезов МРНП: Прикладная геофизика, вып. 102, с. 37–48).

Best Paper Award Winners

1947

RAYMOND MAILLET
"The Fundamental Equations of Electrical Prospecting"

1949

LEO J. PETERS
"The Direct Approach to Magnetic Interpretation and Its Practical Application"

1950

MILLER QUARLES, JR.
"Fault Interpretation from Seismic Data in Southwest Texas"

1951

LAWRENCE Y. FAUST
"Seismic Velocity as a Function of Depth and Geologic Time"

1952

THEODOR KREY
"The Significance of Diffraction in the Investigation of Faults"

1953

CHARLES B. OFFICER, JR
"The Refraction Arrival in Water-Covered Layers"

"*Silver Anniversary Issue*," *Geophysics*, XXV, 1(1960).